DOI: 10.21917/ijivp.2022.0374

SEGMENTATION OF CAROTID ARTERY FROM INTRAVASCULAR ULTRASOUND (IVUS) IMAGES USING DEEP LEARNING TECHNIQUES FOR PLAQUE IDENTIFICATION

K.V. Archana and R. Vanithamani
Department of Electronics and Communication Engineering, Avinashilingam Institute for Home Science and Higher Education for Women, India

Abstract
The carotid artery is the major artery that supplies blood to the brain, neck region, and face. The plaque deposition in these arteries is caused mainly due to the deposition of cholesterol, calcium, and other cellular debris carried along with the bloodstream. Hence identification of plaque is essential to avoid stroke and other diseases related to the heart. This paper proposes a deep learning-based segmentation algorithm for the identification of plaque in carotid artery using Intravascular Ultrasound (IVUS) images. To compare the performance of the proposed algorithm with the existing algorithms, evaluation metrics such as Jaccard Index (JI), Dice Similarity Coefficient (DC), and Hausdorff Distance (HD) are computed. From the results, it is observed that the proposed algorithm exhibited a high value with JI of 0.9562, DC of 0.9587, and HD of 4.8080.

Keywords:
Intravascular Ultrasound Image, Segmentation, Deep Learning, Jaccard Index, Hausdorff Distance, Dice Coefficient

1. INTRODUCTION

Cardiovascular Disease (CVD) is the leading cause of death, according to the survey by World Health Organisation (WHO). Recent studies show that an estimate of 17.9 million people is affected by CVD in 2019, representing 32% of global deaths. During this pandemic situation, persons with heart problems are highly susceptible to infection. Hence, identifying the plaque deposits plays a vital role in diagnosis of CVDs. The CVD risk factors as stated by WHO are tobacco use, unhealthy dietary practices, alcohol consumption, and insufficient physical activities [12].

The carotid artery has three main layers, namely the inner layer (tunica intima), the middle layer (tunica media), and the outer layer (tunica adventitia). In most cases, the plaque deposition occurs between the inner and the middle layer. This thickening of arterial walls is termed as atherosclerosis. It causes damage to the endothelium layers in the blood vessels. The adverse effect of atherosclerosis is myocardial infarction and stroke [1]. IVUS is a medical imaging technique done in-vivo to acquire tomographic images of the vessel in grayscale [13]. If the plaque deposition gets unnoticed in the carotid artery, it may lead to stroke and causes the insufficient blood supply to the brain: further leading to death. Hence, proper segmentation and identification of plaque is a life-saving process.

In this work, a deep learning method is proposed to segment the boundaries in the IVUS images along with the location of edges. Deep learning models showed excellent performance in segmenting the lumen and the vessel walls [22]. The performance of the proposed method is compared with the existing algorithms like Fuzzy C Means Clustering (FCM), Watershed segmentation, Otsu's thresholding, Gray level thresholding, K means clustering, and Global region-based segmentation. In this paper, longitudinal view of IVUS images is utilized. The proposed method aids physicians for the identification of plaque in the carotid artery.

The rest of the paper is organized as follows, the dataset and the methodology used by researchers for the segmentation of ultrasound images are discussed in detail in section 2. Section 3 discusses the methods used in this work, followed by the results and discussions in Section 4. Section 5 concludes the work.

2. RELATED WORK

This section gives an insight into the different algorithms and methods used for the segmentation. A technique was proposed to identify the link between the deposition of plaque in coronary and the carotid arteries [1]. The dataset comprised of images from 15 subjects using ultrasound B scan and IVUS catheter iMap. The study was based on two hypotheses, the existence of plaque in coronary vessels and analysis of cardiovascular disease by stroke risk biomarker. An active contour approach was used to segment the carotid artery from ultrasound images [2]. The feature vector used for the classification was Intima- Media Thickness (IMT) measurement. Five different features such as average, variance, standard deviation, skewness, and kurtosis were extracted and used to train K-Nearest Neighbors (KNN) classifier. The proposed approach achieved an accuracy of 98.30%, F score of 0.9760 and Matthews Correlation Coefficient (MCC) of 0.9520.

A neural network-based approach was utilized for the segmentation of plaques in carotid arteries [22]. The images were acquired from 189 subjects through T2-weighted Magnetic Resonance Imaging (MRI). The images were divided into two, one to segment the vessel wall and the other to segment the lumen. Two Convolutional Neural Networks (CNN) were used for segmentation process. The performance metrics used were Dice Coefficient, Pearson Correlation, Intra-class Correlation Coefficient (ICC), and Bland-Altman plots. The Dice Coefficient value obtained was 0.96 for lumen and 0.87 for vessel wall, Pearson value was 0.98, and ICC was 0.98 for lumen, and Pearson value was 0.88, and ICC was 0.86 for vessel wall. The segmentation work needed human supervision and monitoring to get reliable, and consistent results. It is found that the layers of adventitia, intima, and media were embedded with plaque and a method was implemented to segment the layers and to detect the outer boundary in the image [3]. Ten images from IVUS dataset B images were utilized for the study. The segmentation used was Otsu thresholding followed by binary-morphological operation and empirical thresholding. In the output image obtained, two coloured images were seen: the red line indicating manual segmentation and the green line depicting automatic segmentation. The Jaccard Index obtained was 0.9106.

In recent years, deep learning-based segmentation is gaining importance because of its robustness and segmentation accuracy. In [22], U-Net architecture model was modified by adding two decoders to detect the shape and edges. IVUS dataset consisting of 118 images were taken from 101 patients, and experienced radiologists annotated them. For training the network, 9715 frames were selected in the final stage. The performance of the proposed model was evaluated by JI, DC, HD, and Percentage of Area Difference (PAD). The model showed excellent performance in segmentation of lumen and vessel areas. A comparative study on various image segmentation techniques using CNN was presented [9]. The paper highlighted the multiple applications of CNN, explaining the various layers and how all the researchers have implemented these layers. An experiment was designed to compare the CNN and Back Propagation Network (BPN) results [18]. Two CNN architecture are designed with two pooled layers, a fully connected layer, and a SoftMax layer for object recognition and segmentation in artery wall image is implemented in [4]. The highest accuracy achieved by CNN was 98.12% which was 1% higher than the BPN. A self-learning-based segmentation technique to extract the edges from the images is proposed in [10]. These extracted edges were given as input to Density-Based Spatial Clustering of Applications with Noise (DBSCAN) for segmentation of pixels. The results were analyzed with Gradient Vector Flow (GVF) snake model and Particle Swarm Optimisation (PSO) model. Three hundred sixty-one longitudinal B-type ultrasound images were utilized in the study. The proposed algorithm was accurate by 12% than the manual segmentation. The Table.1 provides a summary of segmentation techniques.

Table.1. Summary of segmentation techniques

Author	**Input source**	**Segmentation Technique**	**Evaluation Metrics**
Chaudhry et al. [2]	-	Active Contour	Matthews Correlation Coefficient
Mao et al. [20]	-	Contour, Euclidean Distance Map calculation, thresholding.	Mean, Standard Deviation, Sensitivity, Mean Contour Error, Accuracy, Relative Mean Square Error
Sofian et al. [4]	Ten images	Otsu Thresholding	Jaccard Index
Araki et al. [1]	Coronary IVUS and carotid B-mode US	SVM with different kernel type.	Accuracy, Positive Predictive Value, Area Under Curve, Sensitivity, and Specificity.
Latha et al. [4]	361 longitudinal B scan US images	DBSCAN, GVF snake model and PSO Model	-
Mazhar et al. [15]	Case study, extracting images from videos	Contour	Bland-Altman, Linear Regression Parameters.
Zhaode et al. [13]	-	Superpixel-Wise Fuzzy Clustering Technique with Level Set Evaluation	Jaccard Index, Dice Similarity Coefficient and Percentage of Area Difference
Nagaraj et al. [6]	One hundred images, of which 70 are utilized for the study.	Fast edge detection by Random Forest	Mean Absolute Distance Metric, Polyline Distance, Execution Time
Yang et al. [14]	68 IVUS images from 17 patients	Active contour	Dice Similarity Coefficient, Mean Absolute Distance Metric.
Qian [8]	80 B mode longitudinal ultrasound images	SVM with the Kernel, SVM with Radial bias, Adaboost, Random Forest	Sensitivity, Specificity, Dice Similarity Coefficient, Overlap Index, Error of Area, Absolute Error Area, HD, and Point-to-Point distance.

3. METHODOLOGY

This section gives a brief insight into the dataset and methodology used for the study.A comparative study on different algorithms is also discussed in this section.

3.1 IVUS DATASET

IVUS dataset are open source and are made available from Loizou et al. [23]. It consists of 99 images without annotations. The Fig.1 shows the longitudinal slice of the IVUS image dataset. Ground truth image is manually extracted from all the images using the gray-level thresholding technique, and they are used for the training the deep learning network.

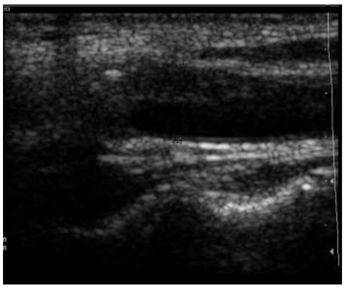

Fig.1. Slice of an image from IVUS dataset

3.2 SEGMENTATION METHOD

The deep learning model used in this study for the segmentation of plaque is CNN. The model consisted of four primary layers, namely, input layer, max-pooling layer, convolutional layer, and SoftMax layer. The filter size used in this work is 5×5. The Fig.2 illustrates the proposed system. An IVUS image is retrieved from a publicly available database.

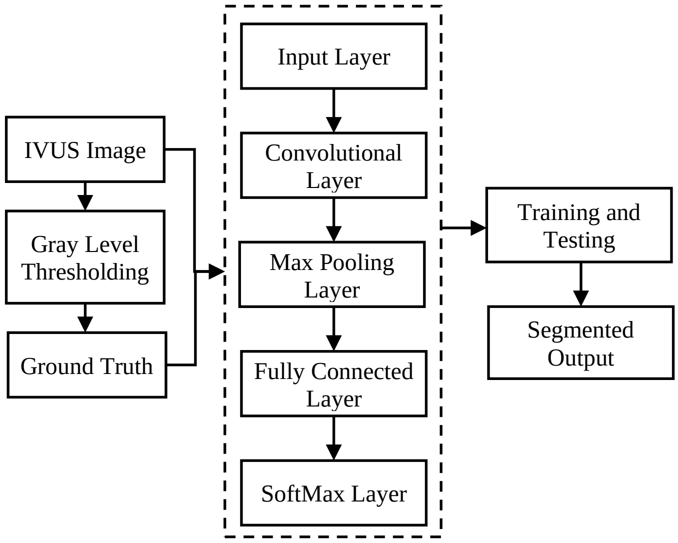

Fig.2. Proposed system

Using gray level thresholding on the input image, the ground truth is calculated. A CNN network is trained with the input image and the ground truth image. A description of the parameters and layers defined in the network can be found in Table.2. Following training, the CNN architecture is tested with a new image, and the segmented output is evaluated by Jaccard Index, Dice Coefficient, and Hausdroff Distance. The step-by-step explanation is provided below,

Step 1: Selecting a sample image from IVUS dataset.

Step 2: Extraction of ground truth image by applying Gray Level threshold to the input image.

Step 3: From the dataset of 99 IVUS images, 99 ground truth images were taken. Totally (99 + 99) 198 image dataset is used for training and testing the network.

Step 4: In the CNN, 138 images are used for training and 60 images for testing. The stride value of the pooling layer is set to two, and the filter size is 5×5.

Step 5: Testing is done to validate the performance of the network.

Finally, the segmented image is compared with other algorithms like Active Contour [2] [11] [14], FCM, K Means clustering, Watershed segmentation and Otsu's segmentation using performance metrics.

3.3 CNN ARCHITECTURE

In the architecture of self-designed CNN, the convolutional layer is used to extract the features from the input layer. The convolution operation is performed between the input layer and the filter of desired size. The filter size used in this network is 5×5 (decided based on the number of layers and the feature size). Larger the filter size, more learnable parameter. Hence to design a manageable architecture, 5×5 filter size is chosen. The output of the convolutional layer, i.e., the feature map is fed to the pooling layer.

In Pooling layer, the feature map size is reduced, thereby reducing the computational cost. In the proposed work, Max polling layer is used to calculate the largest value in the feature map. The pooling layer serves as a connector between the convolution layer and the Fully Connected (FC) layer.

In the FC layer, different neuron connections are made. The training phase begins at this level. The activation function included in this network, is the ReLU and SoftMax. This layer adds non-linearity to the network.

The training set consists of 138 images including the original image and the ground truth image. The Table.2 shows the CNN Architecture parameters. The architecture consists of one Convolutional layer of 96 kernels, one Pooling layer, FC layer size 4096×1 with zero Padding. The size of the input image is 227×227. Convolutional layer is the primary layer with tensor size of 55×55×96, weight of 34,848 and bias of 96. The Fully Connected Layer uses a tensor size of 4096×1, and the Softmax Layer uses a size of 1000×1.

Table.2. CNN Architecture parameters

Layer Name	Tensor Size	Weights	Bias	Parameters
Input	227×227×3	0	0	0
Convolution	55×55×96	34,848	96	34,944
Max Pool	27×27×96	0	0	0
FC	4096×1	37,748,736	4096	37,752,832
SoftMax	1000×1	0	0	0

The Table.3 discusses the hyper parameters used for the tuning of CNN architecture. A CNN architecture is designed using two activation functions: SoftMax and ReLU. 0.0001 is set as the learning rate of the system. Stochastic Gradient Descent with Momentum (SGDM) is the optimizer employed in the system. The size of the mini-batch is 125, the epoch is 20, and there are 100 hidden neurons in the system.

Table.3. Hyper parameter tuning in CNN Architecture

Parameters	Specifications
Activation Function	ReLU and SoftMax
Learning Rate	0.0001
Optimiser	Stochastic Gradient Descent with Momentum (*SGDM*)
Mini - Batch Size	125
Epochs	20
No. of Hidden Neurons	100
Fully Connected Layers	2

4. PERFORMANCE MEASURES

The automatic segmentation of IVUS images is compared with the ground truth images using the performance metrics such as JI, HD and DC. Even though image segmentation techniques have advanced greatly, evaluation of these methods has remained largely subjective. A new algorithm's effectiveness is normally demonstrated only by its ability to segment some images that are then evaluated using some method, or by its ability to perform subjectively.

4.1 JACCARD INDEX (JI)

Jaccard similarity coefficient is a measure to identify the similarity between the samples. This work compares the ground truth with the output images from the segmentation algorithms, and the resulting output is tabulated. It is defined by Eq.(1), where *A* and *B* are the vessel regions defined by ground truth and automatic segmentation. Jaccard's similarity coefficient is a statistical measure used to determine whether two sample sets are comparable. The measure focuses on the similarity between finite sample sets, and is formally defined as the intersection of the sets divided by their union.

$$\left|\frac{A_{seg\,img} \cap A_{GT}}{A_{seg\,img} \cup A_{GT}}\right| = JI\left(A_{seg\,img}, A_{GT}\right) \quad (1)$$

where,

$A_{seg\,img}$ = Segmented Image

A_{GT} = Ground Image

4.2 HAUSDORFF DISTANCE

In medical image segmentation, Hausdorff distance is used to calculate the ground truth with the segmented image [19]. Each segmentation is given a ranking and based on these rankings, and the metrics are evaluated for each segmentation algorithms. The Hausdorff distance between two finite set points *X* and *Y* is given in Eq.(2). The directed average Hausdorff distance separating point set (*X* from *Y*) from any point is given by dividing the minimum distances from all points from the point set (*X*) by the number of points in *X*. It is possible to calculate average Hausdorff distance by summing the directed average Hausdorff distances from (*X* to *Y*) and (*Y* to X).

$$d_{HD}\left(X,Y\right) = \frac{1}{2}\left(\frac{1}{X}\sum_{x\in X}\min d\left(x,y\right) + \frac{1}{Y}\sum_{x\in X}\min d\left(x,y\right)\right) \quad (2)$$

4.3 DICE SIMILARITY COEFFICIENT

Slice-by-slice comparison of segmented image to that of ground truth is evaluated using dice similarity coefficient. The overlapping areas of the segmented image are estimated using Eq.(3) [14].

$$DC = 2\frac{\left|A_{seg\,img} \cap A_{GT}\right|}{\left|A_{seg\,img}\right| + \left|A_{GT}\right|} \quad (3)$$

As these metrics accept the input image as binary, all the final segmented images and the ground truth are converted to binary form, and the evaluation is performed. This represents two sets of images (A segment image) and (A original image). The number of elements of a set indicated by vertical bars refers to the cardinality of the set. For example, $|A_{seg\ img}|$ is the number of elements in set $A_{seg\ img}$. An intersection of two sets is represented by a ∩, which means all the elements that both sets have in common

5. RESULTS AND DISCUSSION

Segmentation is essential to detect the plaque in IVUS images. Deep learning-based technique is proved to be efficient in plaque segmentation from the artery wall. The layers of CNN architecture are maintained to be minimal, so that error detection becomes more manageable. The Table.4 compares the performance of the proposed work with the existing algorithms using the metrics such as JI, DC, and HD, implemented for test image 1 and 2. The JI value of 0.956 and DC of 0.9587 is achieved by the proposed method is higher compared to other existing techniques indicating better segmentation of region of interest. The minimal value of HD (4.8080) indicates the closeness of the segmented region to the ground truth image.

Table.4. Comparison of performance using Jaccard Index (JI), Dice Coefficient (DC), and Hausdorff Distance (HD)

Algorithm	Test Image 1			Test Image 2		
	JI	**DC**	**HD**	**JI**	**DC**	**HD**
Watershed	0.9206	0.9014	5.2136	0.9105	0.9101	5.6201
Otsu's Thresholding [3]	0.9012	0.8996	6.7895	0.9089	0.8989	6.0041
K Means *K*=1	0.8456	0.8012	5.7123	0.8956	0.8256	5.8941
K Means *K*=4	0.8899	0.8874	6.9874	0.8664	0.8881	6.9012
FCM [13]	0.8574	0.8791	5.7894	0.8756	0.9008	4.5687
Global Region-based segmentation [20]	0.9100	0.9014	4.9567	0.9075	0.9024	4.9568
Proposed Method	**0.9562**	**0.9587**	**4.8080**	**0.9209**	**0.9156**	**4.4977**

The Fig.3 shows the following: Fig.3(a) and Fig.3(b) are the Test image 1 and 2, Fig.3(c) to Fig.3(p) shows the segenented output obtained by implementing Watershed Segmentation, Otsu's thresholding, *K* means with *k*=1, *K* means with *k*=4, Fuzzy C Means Clustering, Global Region-based segmentation based on Chan-Vese active contour algorithm and finally the proposed deep learning model. In case of *K* means algorithm, with the increase in the *k* value, the output image gets blurred and distorted, hence *k*=1 and *k*=4 is chosen for the analysis. From the segmented images, it is observed that the proposed method is able to segment the artery walls better than the other methods. The contour lines represent the carotid artery walls and different outputs resulting from segmentation algorithms. In terms of JI, DC, and HD results, the proposed model shows promising results. In Fig.3, the output image of the proposed model is shown in sections Fig.3(o) and Fig.3(p). Both the plaque region and the carotid walls are clearly visible in the segmented image.

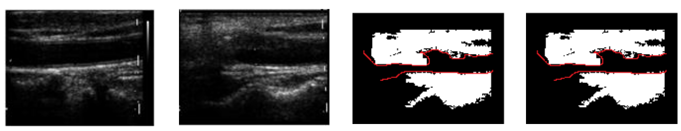

(a) Test Image 1 (b) Test Image 2 (c) Watershed segmentation of Test Image 1 (d) Watershed segmentation of Test Image 2

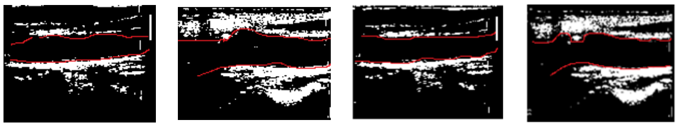

(e) Otsu's Thresholding Test Image 1 | (f) Otsu's Thresholding Test Image 2 | (g) K-Means, k=1 Test Image 1 | (h) K-Means, k=4 Test Image 2

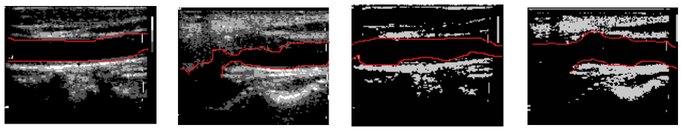

(i) K-Means, k=4 Test Image 1 | (j) K-Means, k=4 Test Image 2 | (k) FCM Test Image 1 | (l) FCM Test Image 2

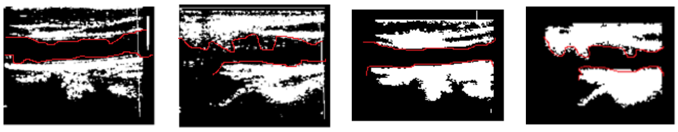

(m) Global Region Segmentation Test Image 1 | (n) Global Region Segmentation Test Image 2 | (o) Proposed Method Test Image 1 | (p) Proposed Method Test Image 2

Fig.3. (a) and (b) are test images, (c)-(p) are the segmented images from implementing Watershed, Otsu's thresholding, K-Means (with k=1 and k=4), FCM, Global Region based and self-designed CNN architecture

Table.5. Average value of Performance Metrics for 60 test images

Algorithm	Test Image Average		
	JI	DC	HD
Watershed	0.9315	0.9078	5.8745
Otsu's Thresholding [3]	0.9056	0.9018	6.8765
K Means K=1	0.8546	0.8002	5.7048
K Means K=4	0.8979	0.8974	6.9910
FCM [13]	0.8574	0.8791	5.1709
Global Region-based segmentation [20]	0.9087	0.9019	4.9669
Proposed Method	**0.9570**	**0.9641**	**4.7980**

The Table.5 gives the average value of the metrics calculated for all the 60 test images. It is observed from the Table.5 that the values of JI (0.9570) and DC (0.9641) calculated from the CNN architecture are close to 1, indicating that the segmented image resembles closer to the extracted ground truth region. The minimal value of HD (4.7980) in proposed method indicates the closeness of the segmented region with the ground truth image. The total execution time is less in CNN architecture compared to the other algorithms implemented.

The work presents a comparison of the techniques used in segmenting the plaque region from the IVUS image. The precise segmentation can help in evaluating the narrowing of the artery wall due to the plaque deposition. Considering the requirement of the analysis, it is observed from the Fig.3, the proposed CNN architecture gives a significant result compared to other techniques. Also, the performance metrics evaluation for the test images signifies the closeness of the segmented region to the ground truth image.

6. CONCLUSION

In this paper, a deep learning-based segmentation is implemented for identifying the plaque deposited regions in arterial wall. Based on the segmented region, physician can decide on the diagnostic procedure to be carried out further. The proposed method implements a CNN structure for segmenting the plaque region using an IVUS image dataset. Initially, ground truth data is extracted through grey- level thresholding. CNN architecture is trained with dataset of 138 images and tested with 60 images. The performance metrics includes JI, DC and HD and compared with other existing algorithms. From the analysis, it is noted that the values of JI and DC are highly close to the value of one compared to other segmenting algorithms. This indicates that the segmented regions are closer to the ground truth, resulting in better segmentation of the Region of Interest. The work can be further extended in classifying the types of plaques and indicating the level of narrowing of artery wall. This in turn will aid the physician in deciding on the type of treatment procedure to be carried further.

REFERENCES

[1] Tadashi Araki, Nobutaka Ikeda, Devarshi Shukla, Narendra D Londhe, Vimal K Shrivastava, Sumit K Banchhor, Luca Saba, Ardrew Nicolaides, Shoaib Shafique, John R Laird and Jasjit S Suri, "A New Method for IVUS-based Coronary Artery Disease Risk Stratification: A Link between Coronary and Carotid Ultrasound Plaque Burdens", *Computer Methods and Programs in Biomedicine*, Vol. 124, pp. 161-179, 2015.

[2] A. Chaudhry, M. Hassan, A. Khan, J.Y. Kim and T.A. Tuan, "Automatic Segmentation and Decision Making of Carotid Artery Ultrasound Images", *Proceedings of International Conference on Advances in Intelligent Systems and Computing*, pp. 1-13, 2013.

[3] Hannah Sofian, C.M. Joel, Norliza Mohd Noor and Hassan Dao, "Segmentation and Detection of Media Adventitia Coronary Artery Boundary in Medical Imaging Intravascular Ultrasound Using Otsu thresholding", *Proceedings of International Conference on Bio Signal Analysis, Processing and Systems*, pp. 1-13, 2015.

[4] S. Latha, D. Samiappan and P. Muthu, "Fully Automated Integrated Segmentation of Carotid Artery Ultrasound Images using DBSCAN and Affinity Propagation", *Journal of Medical and Biological Engineering*, Vol. 41, pp. 260-271, 2021.

[5] C. Loizou and Marios Pantzaris, "Atherosclerotic Carotid Plaque Segmentation in Ultrasound Imaging of the Carotid Artery", *Proceedings of International Conference on Multi-Modality Atherosclerosis Imaging and Diagnosis*, pp. 233-238, 2014.

[6] Y. Nagaraj, C.S. Asha, A. Hema Sai Teja and A.V. Narasimhadhan, "Carotid Wall Segmentation in Longitudinal Ultrasound Images using Structured Random Forest", *Computers and Electrical Engineering*, Vol. 69, pp. 753-767, 2018.

[7] V. Naik, R.S. Gamad and P.P. Bansod,"Carotid Artery Segmentation in Ultrasound Images and Measurement of

Intima-Media Thickness", *BioMed Research International*, Vol. 2013, pp. 1-15, 2013.

[8] C. Qian and X. Yang, "An Integrated Method for Atherosclerotic Carotid Plaque Segmentation in Ultrasound Image", *Computer Methods Programs Biomedicine*, Vol. 153, pp. 19-32, 2018.

[9] Ravi Kaushik and Shailender Kumar, "Image Segmentation using Convolutional Neural Network", *International Journal of Scientific and Technology Research*, Vol. 8, No. 11, pp. 1-9, 2019.

[10] S. Latha, Dhanalakshmi Samiappan and R. Kumar, "Carotid Artery Ultrasound Image Analysis: A Review of the Literature", *Proceedings of the Institution of Mechanical Engineers, Part H: Journal of Engineering in Medicine*, pp. 1-8, 2020.

[11] M. Tayel and Y. Farouk, „A Modified Segmentation Method for Determination of IV Vessel Boundaries", *Alexandria Engineering Journal*, Vol. 23, No. 1, pp. 1-22, 2017.

[12] World Health Organisation, "Cardiovascular Diseases (CVDs)", Available at www.who.int/news-room/fact-sheets/detail/cardiovascular-diseases-(cvds), Accessed at 2021.

[13] Z. Xia, Z. Zhaoyu and Z. Wang,"IVUS Image Segmentation using Superpixel-Wise Fuzzy Clustering and Level Set Evolution", *Applied Sciences*, Vol. 43, No. 1, pp. 1-15, 2019.

[14] Xin Yang, Jiaoying Jin, Mengling Xu, Huihui Wu, Wanji He, Ming Yuchi and Mingyue Ding, "Ultrasound Common Carotid Artery Segmentation Based on Active Shape Model", *Computational and Mathematical Methods in Medicine*, Vol. 2013, pp. 1-12, 2013.

[15] J. Yang, L. Tong and A. Basu, "IVUS-Net: An Intravascular Ultrasound Segmentation Network", *Proceedings of International Conference on Smart Multimedia*, pp. 1-13, 2015.

[16] M. Ziegler, J. Alfraeus and M. Bustamante, "Automated Segmentation of the Individual Branches of the Carotid Arteries in Contrast-Enhanced MR Angiography Using Deep Medic", *BMC Med Imaging*, Vol. 38, pp. 1-15, 2021.

[17] P. Ziemer, C. Bulant, J. Orlando and P. Blanco,"Automated Lumen Segmentation Using Multi-Frame Convolutional Neural Networks in Intravascular Ultrasound Datasets", *European Heart Journal - Digital Health*, Vol. 2020, pp. 1-11, 2020.

[18] Z. Zhou, H. Wang, W. Shang and L. Zhang, „Image Segmentation Algorithms Based on Convolutional Neural Networks", *Proceedings of International Conference on Computer and Information Science*, pp. 1-13, 2018.

[19] O.U. Aydin, A.A. Taha and A. Hilbert,"On the Usage of Average Hausdorff Distance for Segmentation Performance Assessment: Hidden Error When Used for Ranking", *European Radiology Experimental*, Vol. 5, pp. 1-16, 2021.

[20] P. Getreuer,"Chan-Vese Segmentation", *Image Processing on Line*, Vol. 2, pp. 214-224, 2012.

[21] D.D. Samber, S. Ramachandran and V. Mani, "Segmentation of Carotid Arterial Walls Using Neural Networks", *World Journal of Radiology*, 2020.

[22] J.E. Park, K. Jihoon, A. Pil and Y.H. Kim, "Deep Learning Segmentation of Lumen and Vessel on IVUS Images", *Journal of the American College of Cardiology*, Vol. 77, No. 14, pp. 1-10, 2021.

[23] C.P. Loizou, C.S. Pattichis , M. Pantziaris and A. Nicolaides. "An Integrated System for the Segmentation of Atherosclerotic Carotid Plaque", *IEEE Transactions on Information Technology in Biomedicine*, Vol.11, pp. 1-17, 2007.